Creating a Digital Twin to Investigate AV Block: In-sights From a Validated Electromechanical Full-Heart Model

Kevin L Sack[1], Joshua J Blauer[1], Michael P Campbell[1], Darrell J Swenson[1]

[1]Medtronic Inc, Mounds View MN, United States of America

Abstract

Advancements in computational techniques will soon enable the use of anatomically realistic virtual models to contribute towards regulatory evidence. In this study we introduce methods to construct and validate a subject-specific four-chamber porcine heart model suitable to investigate coupled electro-mechanical phenomena from in vivo data.

Our geometrically detailed, electromechanical four-chamber heart was mechanically calibrated to match the experimentally recorded LV pressure-volume loop. Surfaces of the LV and RV from the model were validated against surfaces extracted from in vivo CT scans, which correlated well (R^2=0.94, 0.95 respectively) over all phases. Validated model function is compared with simulations of AV block in the same subject.

Our findings show that in addition to interrupted flow, AV block creates elevated stress and strain throughout the heart during diastole following the missed ventricular beat. The ventricles, unable to unload, are subjected to increased pressures and volumes which peak during the atrial kick. At this point mean ventricular stress were elevated by 50% (3.0 vs. 4.5 kPa, normal vs. AV block).

Our study validates an electromechanical four-chamber heart model and demonstrates model utility to investigate pathology using a "digital twin".

1. Introduction

Computational modelling is an emergent field of research within the cardiac biomedical community that has the potential to rapidly accelerate the process of identifying viable therapies, improving therapy design, advancing medical device performance and safety, and optimizing patient selection. Advancements of computational techniques and resources are enabling researchers to create highly detailed patient- and subject-specific cardiac models that behave as "digital twins" to their physiological counterparts [1]. This paves the way for virtual clinical trials, whereby anatomically identical, computer-generated models would be used for regulatory evidence [2]. As an initial assessment of efficacy and safety, modelling could substantially reduce the risk to individuals and animals involved in therapy trials. This would also improve the rigor of medical device assessment and save significant costs associated with clinical testing and validation.

In this study we introduce methods to construct and validate a subject-specific four-chamber porcine heart model suitable to investigate coupled electro-mechanical phenomena from *in vivo* data. Normal heart function is simulated and compared with simulations of atrioventricular (AV) block in the same subject.

2. Methods

2.1. Experimental methods

A female Yorkshire-mix domestic swine, body weight of 99 kg, with an ablated AV node and an investigational Micra AV ™ pacing device implanted in the right ventricle was used for this study. Subject was sedated (Midazolam 38 mg, Butorphanol 38 mg, Xylazine 290 mg; IM) and surgical anaesthesia was maintained with isoflurane 1.6–2.6%. Subject was arranged in supine position whereby AV synchrony and heart function was confirmed normal with Echocardiogram prior 10 phase CT image acquisition and pressure catheter data collection was performed.

2.2. Geometric segmentation

CT scan data were imported and processed in Simpleware ScanIP (Synopsys, Mountain View, USA). Detailed geometric segmentations of the atria and the ventricles at end diastole were created and meshed into 10-node tetrahedral elements. Inner surfaces of the left ventricle (LV) and right ventricle (RV) for each of the 10 phases of the cardiac cycle were also segmented and set aside for validation purposes.

2.3. Myofiber orientations

Myofiber orientation in the ventricular structure has been well described in the literature [3]. Accordingly, we assumed that the ventricular myofiber orientation could be represented through a linearly varying helix angle from −60° on the epicardium to +60° on the endocardium. Myofiber orientations of papillary structures and the extending pulmonary trunk were assigned manually to

run parallel and circumferential to anatomical structures respectively. Myofiber orientations in the atria are characterized by overlapping, joining and separating fiber bundles that are critical for both electrical and mechanical function [4]. Accordingly, we assigned atrial myofibers aligned circumferentially with the native orifices and atrioventricular valve annuli. Distinct fiber bundles representing Bachman's bundle, pectinate muscle and atrial free wall were prescribed following the morphology of atrial anatomy.

2.4 Constitutive modeling

The passive material response for myocardium is governed by an anisotropic hyperelastic description [5]. Contractile function is coupled to the solution of simulated electrophysiological activation, which is initiated when the calcium transients exceed a resting threshold. Active tension development following initiation is governed by a time varying elastance law [6].

2.5 Excitation contraction coupling

The electrical activation of the heart was simulated using CARP electrophysiology simulation software. The geometry was refined to a tetrahedral mesh with approximately 400 μm edge length resolution. Atrial activation was initiated from the sinoatrial node, and the ventricles were paced at the embedded Micra location. The cardiac activation was simulated in a pseudo-bidomain mode for atrial [7] and ventricular [8] cell models. The calcium transients for 4 consecutive cycles of activation at a HR of 55 BPM (based on experimentally recorded HR) were exported from the cell models to drive the timing of atria and ventricular contraction. Mechanical coupling was triggered by rapid uptake of calcium transients which initiates active tension development in the time varying elastance law.

2.6. Circulatory system

Our electromechanical four-chamber heart is coupled to a closed loop circulatory model adapted from simple lumped parameter representations of the cardiovascular system [3], shown in Figure 1. Here the atria and ventricular chambers are defined as enclosed fluid-filled cavities where compliance is inherently derived from the material description of the engulfing 3D model of the myocardium. This dictates the pressure-volume (PV) relation of each chamber. Unidirectional fluid exchange, driven by pressure difference between two connected chambers, allow for a meaningful representation of the entire circulatory system and the cyclic performance of a beating heart.

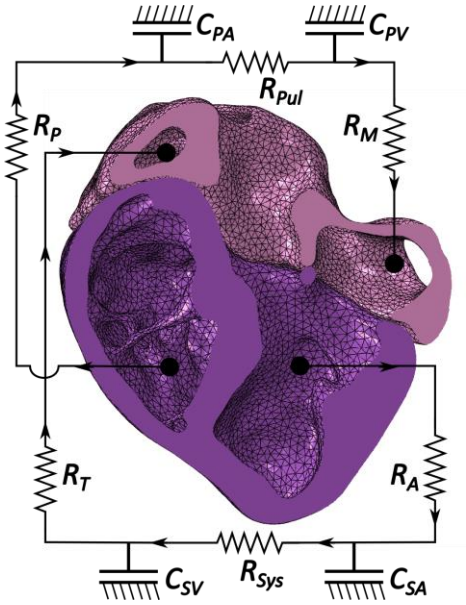

Figure 1. Schematic illustrating the connection between the electromechanical four-chamber heart and the lumped circulatory system composed of compliance and resistance terms.

2.7. Boundary conditions

The vena cava and pulmonary veins restrict motion in the right and left atria respectively. We fixed these orifices to prevent rigid body motion and ensure the model is mathematically well posed. To avoid placing overly restrictive constraints, we enforced a weighted average restraint on the nodes of the abovementioned orifices such that the average deformation around the orifice centre of mass is zero. This averaged constraint method allows for orifice expansion and contraction during the heart cycle, but "centres" motion on a fixed point in space, preventing rigid body motion.

2.8. Stress-free configuration

As both the boundary conditions (including chamber pressure) and the deformed configuration are known, the stress-free configuration is obtainable. This was successfully achieved using an augmented iterative inverse method [9], allowing the resulting unloaded configuration to coincide with the end-diastole configuration at end-diastole loading conditions.

2.9. Calibration

To match the in vivo stroke volume and LV pressure development, the material parameters of the time varying elastance law were determined heuristically along with the compliance and resistance parameters of the lumped circulatory model. This ensures that the *in silico* PV loop

conforms to the *in vivo* determined PV loop.

2.10. Model validation

To validate the model, surfaces of the LV and RV from the *in silico* model were compared to corresponding segmented surfaces from the *in vivo* CT scans. Metrics governing the surface correlation (R^2) and mean distance error were used to validate that simulated cardiac function replicates *in vivo* function to a satisfactory degree.

Mean distance error = $\frac{1}{n}\sum_i^n \sqrt{(p_i - q_i)^2}$, where p_i are control point landmarks on the FEM surface and q_i are the nearest points on the CT surface. Metric of correlation is given by, $R^2 = 1 - \sum_i (p_i - q_i)^2 / \sum_i (r_i - \bar{r})^2$, where r_i are radii lengths at each point landmark and $\bar{r}$ is the mean radial distance of the surface.

2.11. Simulation of AV Block

To model AV block, every other cardiac cycle will exclude EP activation of the ventricular tissue, resulting in a 2:1 ratio of activation. Comparison of peak stress in heart during the skipped beats will be used to quantify the mechanical effect of pathology.

3. Results and discussion

3.1. Hemodynamics

Model function was calibrated to recorded functional metrics. Comparison of the PV loops is given in Figure 2 and the resulting metrics are presented in Table 1.

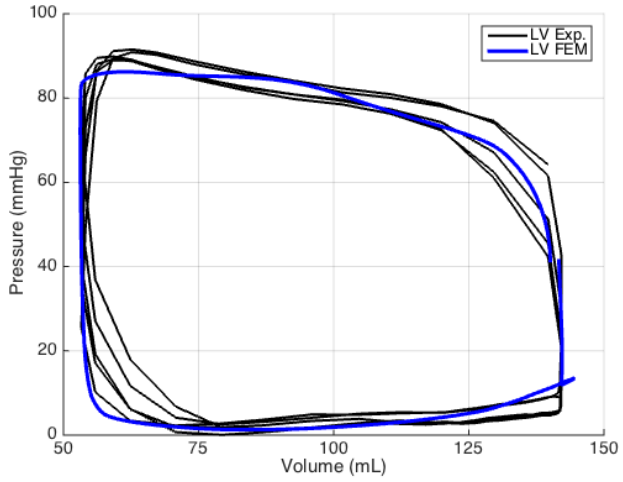

Figure 2. Experimentally (Exp) measured LV PV loop (black line) over 5 beats plotted alongside the *in silico* (FEM) derived PV loop (blue line).

Table 1. Comparison between simulated and experimentally recorded metrics of timing and function

Metric	unit	In silico	In vivo	error	error %
EDV	mL	143.4	142.1	+1.3	0.9 %
ESV	mL	53.3	53.3	+0.04	0.1 %
EDP	mmHg	11.9	11.0	0.9	8.2 %
ESP	mmHg	83.0	86.0	-3.0	-3.5 %
SV	mL	90.1	88.8	1.3	1.5 %
EF	%	62.8	62.5	0.3	0.5 %
HR	Bpm	55	55	0	0.0 %

3.2. Validation

Both LV and RV surfaces correlated well with CT scan surfaces throughout the cardiac cycle (Table 2). Mean R^2 values over the cardiac cycle were 0.94 and 0.95 for the LV and RV respectively.

Table 2. Agreement between LV and RV surfaces from calibrated model and corresponding CT scan segmentations aligned by scan phase.

Scan phase	LV R^2	LV mean error (mm)	RV R^2	RV mean error (mm)
1	0.95	1.7	0.96	2.1
2	0.90	2.5	0.95	2.9
3	0.91	2.7	0.92	3.4
4	0.92	2.6	0.90	3.7
5	0.85	3.4	0.93	3.1
6	0.92	2.3	0.95	2.5
7	0.96	1.6	0.96	2.0
8	0.98	1.0	0.96	2.0
9	0.99	0.8	0.96	2.0
10	0.98	1.2	0.98	1.8

3.2. Measured effect of AV block

Activation patterns throughout our whole heart model are illustrated over a single beat in Figure 3 for normal and AV block simulations. The ventricles, unable to unload, are subjected to increased pressures (Figure 3) and volumes which peak during the atrial kick following the missed ventricular beat. In addition to the hemodynamic consequences of AV block, (i.e. missed ventricular ejection and interrupted flow), AV block creates elevated stress and strain throughout the heart during the subsequent diastole, peaking during the atrial kick into the overly loaded ventricles. At this point (~2.7s, Figure 3) mean ventricular stress were elevated by 50% (3.0 vs. 4.5 kPa, normal vs. AV block).

The physiological mechanisms that regulate cardiac output and myocyte function are likely disrupted by the

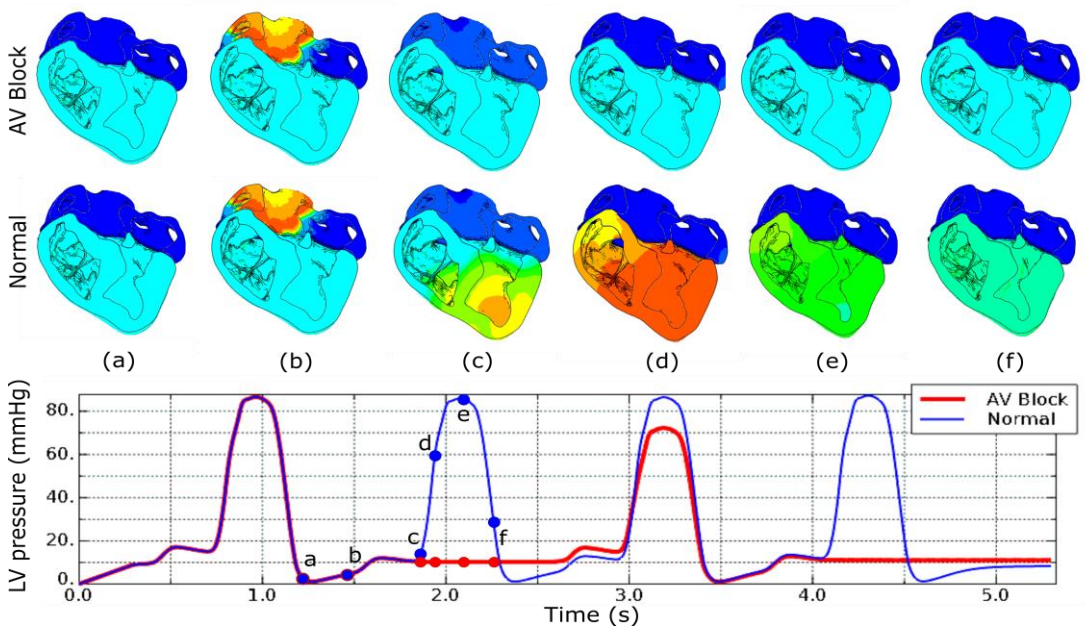

Figure 3: Triggering activation in the normal (middle) and AV block (top) electromechanically coupled full heart model over a complete cycle. Timing events (a-f) correspond to positions marked in left ventricle pressures (bottom).

elevated stress, increased diastolic pressure and the absence of ventricular ejection, which occurs frequently in AV block patients. Without intervention, compensatory adaptations will follow to maintain cardiac output at the expense of long-term cardiac health.

4. Conclusion

Our study validates the electromechanical function of a four-chamber beating heart model and illustrates how a "digital twin" can be used to investigate pathological dysfunction. Comparisons between normal, validated function against pathological states in a computational model provides otherwise unobtainable insights into changes in the electrical, mechanical and hemodynamic function. Utilizing digital twins as a research tool could accelerate the development of emerging therapeutic interventions and enable patient-specific solutions.

Acknowledgments

Authors would like to thank Peter Zhang and Christian Fjeldsted for their assistance towards this study.

References

[1] J. Corral-Acero *et al.*, "The 'Digital Twin' to enable the vision of precision cardiology," *Eur. Heart J.*, Mar. 2020.

[2] M. Reiterer *et al.*, "Advancing regulatory science with computational modeling for medical devices at the FDA's Office of Science and Engineering Laboratories: Computational modeling of medical devices at FDA," *Front. Med.* vol. 5, 2018.

[3] K. L. Sack *et al.*, "Construction and validation of subject-specific biventricular finite-element models of healthy and failing swine hearts from high-resolution DT-MRI," *Front. Physiol.*, vol. 9, p. 539, May 2018.

[4] J. Zhao *et al.*, "An image-based model of atrial muscular architecture," *Circ. Arrhythmia Electrophysiol.*, vol. 5, no. 2, pp. 361–370, Apr. 2012.

[5] G. A. Holzapfel and R. W. Ogden, "Constitutive modelling of passive myocardium: A structurally based framework for material characterization," *Philos. Trans. R. Soc. A Math. Phys. Eng. Sci.*, vol. 367, no. 1902, pp. 3445–3475, Sep. 2009.

[6] J. C. Walker *et al.*, "MRI-based finite-element analysis of left ventricular aneurysm," *Am. J. Physiol. - Hear. Circ. Physiol.*, vol. 289, no. 2 58-2, Aug. 2005.

[7] M. Courtemanche *et al.*, "Ionic targets for drug therapy and atrial fibrillation-induced electrical remodeling: Insights from a mathematical model,".

[8] K. H. W. J. Ten Tusscher *et al.*, "A model for human ventricular tissue," *Am. J. Physiol. - Hear. Circ. Physiol.*, vol. 286, no. 4 55-4, 2004.

[9] M. K. Rausch *et al.*, "An augmented iterative method for identifying a stress-free reference configuration in image-based biomechanical modeling," *J. Biomech.*, vol. 58, pp. 227–231, Jun. 2017.

Address for correspondence:

Kevin L Sack
8200 Coral Sea St NE, Mounds View, MN 55112, United States
Kevin.L.Sack@medtronic.com